Inhibitor-induced structural change of the active site of human poly(ADP-ribose) polymerase

Takayoshi Kinoshita[a,*], Isao Nakanishi[a,1], Masaichi Warizaya[a], Akinori Iwashita[b], Yoshiyuki Kido[c], Kouji Hattori[c], Takashi Fujii[a]

[a] *Exploratory Research Laboratories, Fujisawa Pharmaceutical Co. Ltd., 5-2-3, Tokodai, Tsukuba, Ibaraki 300-2698, Japan*
[b] *Medicinal Biology Research Laboratories, Fujisawa Pharmaceutical Co. Ltd., Kashima 2-1-6, Yodogawa-ku, Osaka 532-8514, Japan*
[c] *Medicinal Chemistry Research Laboratories, Fujisawa Pharmaceutical Co. Ltd., Kashima 2-1-6, Yodogawa-ku, Osaka 532-8514, Japan*

Received 7 October 2003; revised 17 November 2003; accepted 17 November 2003

First published online 28 November 2003

Edited by Hans Eklund

Abstract The crystal structure of human recombinant poly(ADP-ribose) polymerase (PARP) complexed with a potent inhibitor, FR257517, was solved at 3.0 Å resolution. The fluorophenyl part of the inhibitor induces an amazing conformational change in the active site of PARP by motion of the side chain of the amino acid, Arg878, which forms the bottom of the active site. Consequently, a corn-shaped hydrophobic subsite, which consists of the side chains of Leu769, Ile879, Pro881, and the methylene chain of Arg878, newly emerges from the well-known active site.

Key words: Poly(ADP-ribose) polymerase; Inhibitor induced; Crystal structure; Synchrotron radiation; Molecular–molecular interaction; Structural change

1. Introduction

Poly(ADP-ribose) polymerase (PARP: EC 2.4.2.30), a eukaryotic DNA-binding enzyme that participates in cell recovery from DNA damage [1], consists of three functional domains: an N-terminal DNA-binding domain, a C-terminal catalytic domain (catPARP) and a central automodification domain [2]. PARP binds to and is activated by DNA strand breaks and catalyzes the synthesis of homopolymers of ADP-ribose from nicotinamide adenine dinucleotide (NAD^+) onto nuclear acceptor proteins. PARP itself is the main protein acceptor (automodification), but the enzyme has also been shown to modify histones, topoisomerases, DNA polymerases and ligases [3]. The formation of these negatively charged polymers in the vicinity of the DNA nick is thought to cause electrostatic repulsion of PARP from the DNA and to facilitate recruitment of the base excision repair complex [4]. The ADP-ribose polymers formed by PARP are cleaved by the cellular hydrolase poly(ADP-ribose) glycohydrolase. PARP activation and the rapid synthesis and degradation of ADP polymers can result in abrupt and profound cellular NAD^+ depletion.

Cytotoxic drugs or radiation can induce activation of PARP, and it has been demonstrated that inhibitors of PARP can potentiate the DNA-damaging and cytotoxic effects of chemotherapy and irradiation [5]. Because of the essential function of PARP for cellular repair and survival, evaluation of the potential of novel, potent PARP inhibitors for the treatment of cancer in combination with selected cytotoxic agents has been sought. These inhibitors have been designated to mimic the substrate–protein interactions of NAD^+ and PARP using the crystal structure of chicken catPARP [6–8]. The active site of PARP is very large and can be generally classified into two sites: the acceptor site and the donor site [6]. The acceptor site is occupied by the ADP moiety of the poly(ADP-ribose) chain. The donor site is occupied by NAD^+, and conveniently classified into the three subsites consisting of the nicotinamide-ribose binding site (NI site), the phosphate binding site (PH site) and the adenine-ribose binding site (AD site). Known inhibitors bind to the NI site, partially bind to the acceptor site and do not bind to the PH site and/or AD site. FR257517 (Fig. 1), 2-{3-[4-(4-fluorophenyl)-3,6-dihydro-1(2H)-pyridinyl]propyl}-8-methyl-4(3H)-quinazolinone, a potent inhibitor with an IC_{50} value of 14 nM, has a quinazolinone part as a nicotinamide mimic moiety. It is strongly suggested that the quinazolinone part of the inhibitor binds to the NI site based upon structural studies up to this point. The other part of the inhibitor is unique and much larger than other known inhibitors. Based upon a docking study, it was assumed that the inhibitor cannot bind to the acceptor site and/or the AD site without an enforced molec-

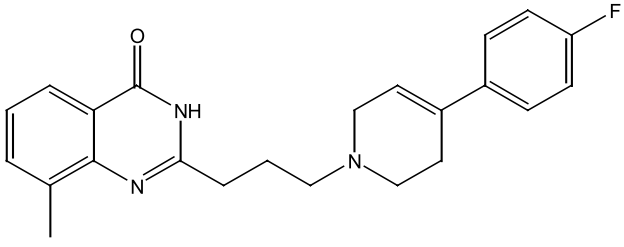

Fig. 1. Chemical structure of FR257517 as a potent inhibitor.

*Corresponding author. Fax: (81)-29-847 8313.
E-mail address: takayoshi_kinoshita@po.fujisawa.co.jp (T. Kinoshita).

[1] Present address: Department of Theoretical Drug Design, Graduate School of Pharmaceutical Science, Kyoto University, Sakyo-ku, Kyoto 606-8501, Japan.

Abbreviations: PARP, poly(ADP-ribose) polymerase; catPARP, C-terminal catalytic domain of poly(ADP-ribose) polymerase; NAD^+, nicotinamide adenine dinucleotide; RMSD, root mean square deviation

0014-5793/03/$30.00
doi:10.1016/S0014-5793(03)01362-0

ular-kink. Thus, it was proposed that FR257517 induces a structural change to the active site of PARP when the inhibitor binds. In order to clarify this hypothesis, we performed an X-ray analysis of the catalytic domain of human catPARP complexed with FR257517.

2. Materials and methods

The human catPARP gene corresponding to amino acid numbers 654–1016 was PCR amplified with a fused protein, glutathione S-transferase, and a thrombin cleavage site. Luria broth medium was inoculated with the DH5α *Escherichia coli* strain containing the catPARP construct. The cells were harvested by centrifugation. The suspension was sonicated and cell debris was removed by centrifugation. The supernatant was purified with a glutathione Sepharose 4B (Amersham Pharmacia) incubated after addition of thrombin. The catPARP protein was concentrated and loaded onto a Superdex 200 HR (Amersham Pharmacia) size-exclusion column. Homogeneous protein was purified from this column by isocratic elution with buffer: 50 mM Tris–HCl, 150 mM NaCl, 1.5 mM dithiothreitol at pH 7.5. The inhibitor FR257517 was suspended in the protein solution. The excess inhibitor was removed by centrifugation before crystallization. Initial crystals were obtained by the hanging-drop vapor-diffusion method using a Crystal Screen kit (Hampton Research). Crystals were obtained under the No. 39 conditions, which were refined using the sitting-drop vapor-diffusion method. The best crystals were obtained using 4 μl of complex solution, which was mixed with 4 μl mother liquor containing 2.1–2.2 M ammonium sulfate, 2% PEG400, 0.1 M Tris–HCl at pH 8.5. Details of the purification and crystallization procedure have been described elsewhere [9].

The crystal was mounted in a nylon loop (Hampton Research) and cooled to 100 K in a nitrogen gas stream. Diffraction dataset was collected at beamline 6B (Photon Factory) using an imaging plate detector [10]. A wavelength of 1.00 Å and a crystal-to-detector distance of 573 mm were used. Data integration was performed with DENZO and scaling and merging were performed using SCALEPACK; both programs are from the HKL program package [11]. The structure was solved by the molecular replacement method using the program AMoRe [12] in the CCP4 program suite. The homology model calculated based upon chicken catPARP was used as a search probe. The program Quanta (Accelrys) was used for model building and CNX (Accelrys) for structure refinement. To obtain the conformation of FR257517 in binding to the protein, several different conformations that fit the residual density in the electron density omit map were subjected to geometrical optimization using the CHARMm force field and CHARMm minimization module of Quanta (Accelrys). The coordinates have been deposited with the Protein Data Bank (accession code is 1UK0).

3. Results and discussion

Human catPARP crystallized in space group $C2$ with unit cell dimensions of $a = 179.82$ Å, $b = 53.55$ Å, $c = 92.01$ Å, and $\beta = 114.4°$ and with two molecules in the asymmetric unit. The final model including two inhibitors, one inhibitor per PARP molecule, has been refined to 3.0 Å. Several amino acids, eight amino acids from the N-terminus and five amino acids from the C-terminus, were omitted from the final model because of ambiguous or discontinuous electron density for the corresponding regions. However, both terminal portions are located at the opposite side of the active site and are irrelevant to the enzymatic activity. The R factor and the root mean square deviation (RMSD) bond lengths and angles reveal a rather low accuracy, but structural features involving inhibitor–protein interaction can be extracted from the final model. Data collection and refinement statistics are summarized in Table 1.

Table 1
Data collection and refinement statistics of the FR257517-catPARP complex

Data collection	
X-ray source	PF/BL6B
Detector system	RAXIS-IV (Rigaku)
Wavelength (Å)	1.00
Space group	$C2$
Cell dimension (Å, °)	$a = 179.82$, $b = 53.55$, $c = 92.01$, $\beta = 114.4$
Resolution range (Å)	30.0–3.0
Number of unique reflections	15 613
Completeness (%)	95.8 (94.7)
R_{merge}[a] (%)	7.5 (24.9)
Refinement	
R_{cryst}[b]/R_{free}[c] (%)	24.0/24.6 (28.3/29.6)
RMSD	
Bond lengths (Å)	0.037
Bond angles (°)	5.5

Values in parentheses refer to the highest shells: 3.18–3.00 Å resolution. RMSD, root mean square deviation.
[a] $R_{merge} = \Sigma_{hkl} |\langle I \rangle - I| / \Sigma_{hkl} |I|$.
[b] $R_{cryst} = \Sigma_{hkl} ||F_{obs}| - |F_{calc}|| / \Sigma_{hkl} |F_{obs}|$, summed over only data (95%) used for refinement.
[c] $R_{free} = \Sigma_{hkl} ||F_{obs}| - |F_{calc}|| / \Sigma_{hkl} |F_{obs}|$, summed over only data (5%) set aside as the test set.

The overall structure of human catPARP is similar to that of chicken catPARP. Thus, architectures of both catPARP are conserved with 0.98 Å RMSD for the Cα atoms of both catPARP (Fig. 2). Furthermore, amino acids around the active site of both PARP species are perfectly conserved, therefore, it is presumed that both PARP species will have a close resemblance when bound by an inhibitor.

The inhibitor could easily fit into the difference electron density map, and this resulted in the inhibitor bound to the active site. Thus, the inhibitor mainly binds to the NI and AD subsites of the donor site, and does not bind the acceptor site

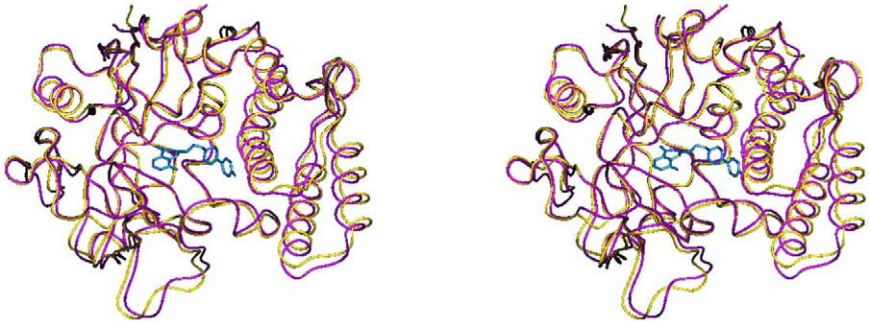

Fig. 2. A stereo view of ribbon diagram of catPARP. Fragments are indicated by color: chicken catPARP (yellow) and human catPARP (purple). The inhibitor (blue) is shown in blue stick form.

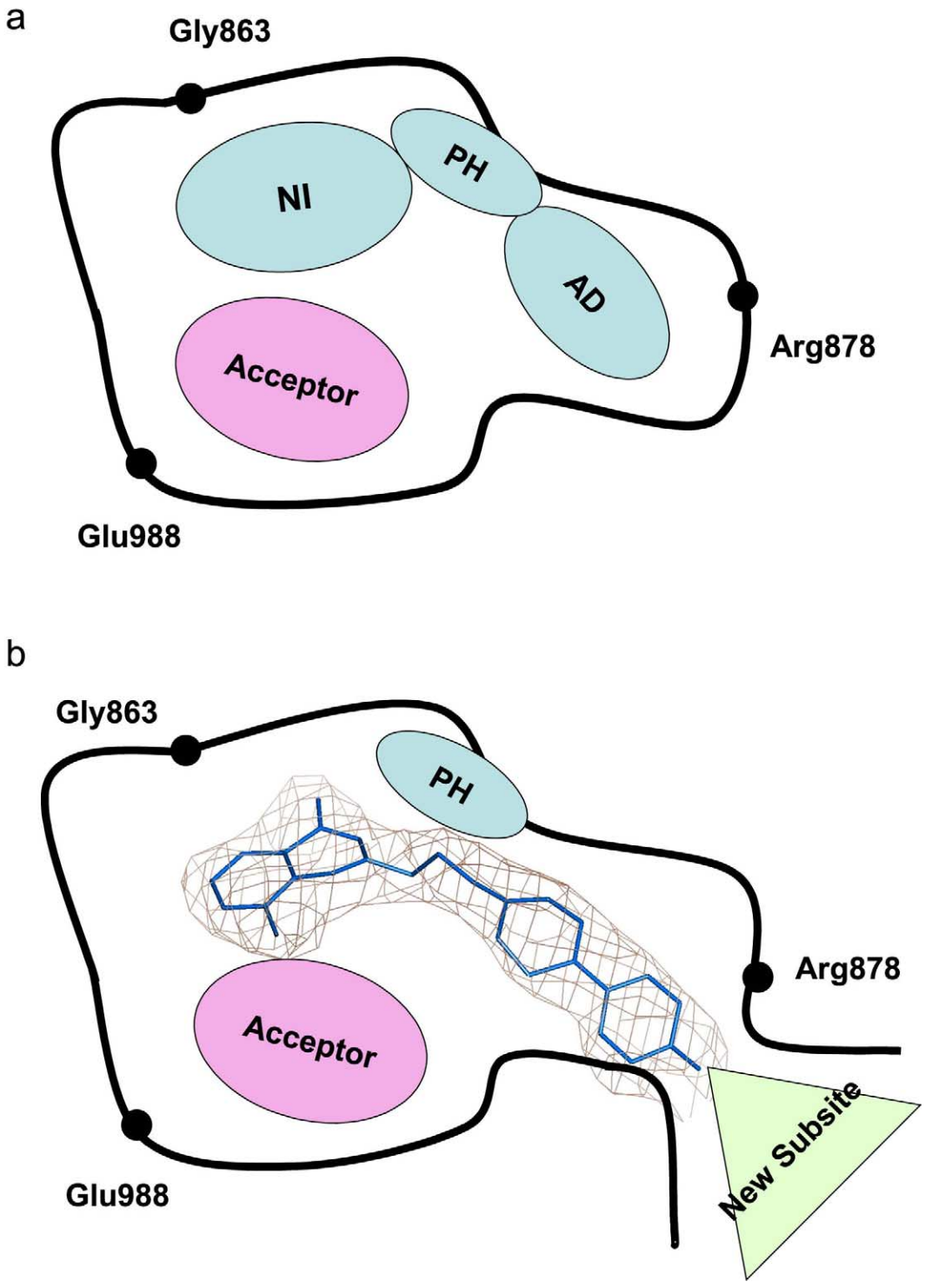

Fig. 3. Illustrated closed-up views of the active site of catPARP with the same orientation as Fig. 2. a: The active site of PARP can be generally classified into two sites: the acceptor site (pink) and the donor site (blue). The acceptor site is occupied by the ADP moiety of the poly-(ADP-ribose) chain. The donor site is occupied by NAD^+, and conveniently classified into the three subsites consisting of the NI site, the PH site and the AD site. b: The inhibitor in the new active site. The inhibitor binds to the NI and AD sites, and the acceptor site and the PH site are unused. The inhibitor also breaks the bottom of the active site wall and produces the hydrophobic corn-shaped subsite.

at all, although known inhibitors utilize the acceptor site. The PH site, highly capable of forming hydrogen bonds, is also unused.

The quinazolinone part of the inhibitor as a nicotinamide mimic moiety tightly binds to the NI site by three hydrogen bonds (C=O to Ser904Oγ and Gly863NH; NH to Gly863-C=O) and by a sandwiched hydrophobic interaction consisting of a π–π interaction with the phenyl ring of Tyr907 and a CH–π interaction with Cβ of Tyr869. The methylene part of the inhibitor, positioning at the place corresponding to di-

phosphate in comparison of chemical structures, does not participate in direct or indirect binding but passes through the PH site. In other words, this part is located at an intermediate position between the acceptor and the donor. It is therefore assumed that the methylene moiety is a spacer to introduce the pyridine moiety and the fluorophenyl group of the inhibitor to the AD site. The pyridine moiety of the inhibitor interacts by van der Waals contacts with Asn767, Asp770, Asp796, Asn868 and Ala880 in the AD site. Additionally, space adjacent to the pyridine moiety remains and a water molecule is located there. The remaining space occupied by the water molecule may be primed for binding of a part of the adenine framework.

It was originally unknown how the fluorophenyl part of the inhibitor induced the conformational change of catPARP, although the adenosine site was too narrow for the binding. It is known that the AD site is at the bottom of the active site and surrounds the adenine moiety at the terminus of substrate NAD^+ (Fig. 3a). Without a conformational change, the fluorophenyl part would cause serious steric-crushes with the protein. Consequently, the fluorophenyl part of the inhibitor induces an amazing conformational change of the AD site. This induced fitting of the inhibitor enlarges the AD site and breaks the bottom of the active site (Fig. 3b). Accordingly, the fluorophenyl group, the terminal part of the inhibitor, can be seen from the opposite side of the active site. Naturally, no portion can be seen from the opposite side of the active site in the known conformation. What is the reason for this large structural change? The backbone structures around the critical portion are fully conserved as mentioned, but the side chain of amino acid Arg878, which forms the bottom of the AD site of the active site, moves greatly upon inhibitor binding. Surprisingly, the motion of a single amino acid induces this large structural change. This also results in generation of a new hydrophobic subsite with a corn shape, consisting of the side chains of Leu769, Ile879, Pro881, and the methylene chain of Arg878.

In summary, we have discovered a novel conformation for catPARP containing a corn-shaped hydrophobic subsite. This observation provides a new concept in inhibitor design using the emerged hydrophobic site, which is located on the opposite side of the active site and therefore has been unused in inhibitor design so far.

Acknowledgements: We would like to thank Dr. Sakabe of Structural Biology Sakabe Project for data collection. We also would like to thank Dr. D. Barrett, Medicinal Chemistry Research Laboratories, for helpful discussion and critical evaluation of the manuscript.

References

[1] Oei, S.L., Griesenbeck, J. and Schweiger, M. (1997) Rev. Physiol. Biochem. Pharmacol. 131, 127–173.
[2] de Murcia, G. and Menissier de Murcia, J. (1994) Trends Biochem. Sci. 19, 172–176.
[3] D'Amours, D., Desnoyers, S., D'Silva, I. and Poirier, G.G. (1999) Biochem. J. 342, 249.
[4] Dantzer, F., Schreiber, V., Neidergang, C., Trucco, C., Flatter, E., De La Rubia, G., Oliver, J., Rolli, V., Menissier-de Murcia, J. and De Murcia, G. (1999) Biochemie 81, 69–75.
[5] Delaney, C.A., Wang, L.Z., Kyle, S., White, A.W., Calvert, A.H., Curtin, N.J., Durkacz, B.W., Hostomsky, Z. and Newell, D.R. (2000) Clin. Cancer Res. 6, 2860–2867.
[6] Ruf, A., Rolli, V., de Murcia, G. and Schulz, G.E. (1998) J. Mol. Biol. 278, 57–65.
[7] White, A.W., Almassy, R., Calvert, A.H., Curtin, N.J., Griffin, R.J., Hostomsky, Z., Maegley, K., Newell, D.R., Srinivasan, S. and Golding, B.T. (2000) J. Med. Chem. 43, 4084–4097.
[8] Koch, S.S.C., Thoresen, L.H., Tikhe, J.G., Maegley, K.A., Almassy, R.J., Li, J., Yu, X.-H., Zook, S.E., Kumpf, R.A., Zhang, C., Boritzki, T.J., Mansour, R.N., Zhang, L.-Z., Ekker, A., Calabrese, C.R., Curtin, N.J., Kyle, S., Thomas, H.D., Wang, L.-Z., Calvert, A.H., Golding, B.T., Griffin, R.J., Newell, D.R., Webber, S.E. and Hostomsky, Z. (2002) J. Med. Chem. 45, 4961–4974.
[9] Kinoshita, T., Tsutsumi, T., Maruki, R., Warizaya, M., Ishii, Y. and Fujii, T., Acta Crystallogr. D, in press.
[10] Sakabe, K., Sasaki, K., Watanabe, N., Suzuki, M., Wang, Z.G., Miyahara, J. and Sakabe, N. (1997) J. Synchrotron Radiat. 4, 136–146.
[11] Otwinowski, Z. and Minor, W. (1997) Methods Enzymol. 276, 307–326.
[12] Navaza, J. (1993) Acta Crystallogr. D49, 588–591.